AD-A065 114 ARMY ELECTRONICS RESEARCH AND DEVELOPMENT COMMAND FO--ETC F/G 14/2
ANALYSIS OF AN INDUCTIVE ENERGY HIGH PERVEANCE ELECTRON BEAM GE--ETC(U)
NOV 78 M WEINER

UNCLASSIFIED DELET-TR-78-31 NL

| OF |
AD
A065114

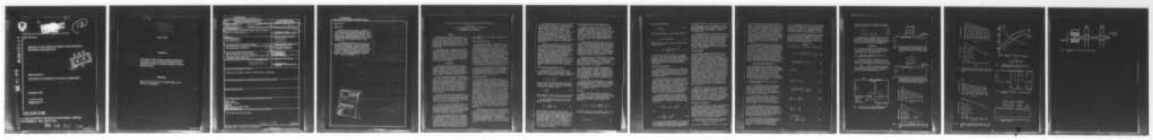

END
DATE FILMED
4-79
DDC

RESEARCH AND DEVELOPMENT TECHNICAL REPORT

DELET-TR-78-31

ANALYSIS OF AN INDUCTIVE ENERGY HIGH PERVEANCE ELECTRON BEAM GENERATOR

Maurice Weiner

ELECTRONICS TECHNOLOGY & DEVICES LABORATORY

November 1978

ERADCOM

US ARMY ELECTRONICS RESEARCH & DEVELOPMENT COMMAND
FORT MONMOUTH, NEW JERSEY 07703

NOTICES

Disclaimers

The citation of trade names and names of manufacturers in this report is not to be construed as official Government indorsement or approval of commercial products or services referenced herein.

Disposition

Destroy this report when it is no longer needed. Do not return it to the originator.

UNCLASSIFIED

SECURITY CLASSIFICATION OF THIS PAGE (When Data Entered)

(14) **REPORT DOCUMENTATION PAGE**

READ INSTRUCTIONS BEFORE COMPLETING FORM

1. REPORT NUMBER: DELET-TR-78-31

2. GOVT ACCESSION NO. (9) Research and development technical

3. RECIPIENT'S CATALOG NUMBER

4. (6) TITLE (and Subtitle): Analysis Of An Inductive Energy High Perveance Electron Beam Generator,

5. TYPE OF REPORT & PERIOD COVERED: Technical Report rept.

6. PERFORMING ORG. REPORT NUMBER

7. (10) AUTHOR(s): Maurice Weiner

8. CONTRACT OR GRANT NUMBER(s): (17) 82

9. PERFORMING ORGANIZATION NAME AND ADDRESS: USA Electronics Technology & Devices Lab. (ERADCOM) Fort Monmouth, NJ 07703

10. PROGRAM ELEMENT, PROJECT, TASK AREA & WORK UNIT NUMBERS: (16) 1L162705AH 94 82 C1

11. CONTROLLING OFFICE NAME AND ADDRESS: Beam, Plasma and Display Division US Army Electronics Technology and Devices Lab (ERADCOM) ATTN: DELET-BG (11)

12. REPORT DATE: Nove[illegible]78

13. NUMBER OF PAGES: 7

14. MONITORING AGENCY NAME & ADDRESS (if different from Controlling Office): (12) 110

15. SECURITY CLASS. (of this report): Unclassified

15a. DECLASSIFICATION/DOWNGRADING SCHEDULE

16. DISTRIBUTION STATEMENT (of this Report)

Approved for public release; distribution unlimitedd.

17. DISTRIBUTION STATEMENT (of the abstract entered in Block 20, if different from Report)

18. SUPPLEMENTARY NOTES

19. KEY WORDS (Continue on reverse side if necessary and identify by block number)

Pulse Power
Nanosecond Pulse
Megavolt
High Energy Electron Beams
High Perveance Gun

20. ABSTRACT (Continue on reverse side if necessary and identify by block number)

See other side for Abstract

410 698

DD FORM 1 JAN 73 1473 EDITION OF 1 NOV 65 IS OBSOLETE

UNCLASSIFIED

SECURITY CLASSIFICATION OF THIS PAGE (When Data Entered)

Block #20

Abstract:

Recently Slivkov and Dolgachev proposed an interesting type of electron beam generator, consisting of a high voltage triode in series with a storage inductor. During the storage time the triode operates with a depressed collector voltage. A high energy current pulse is obtained when the triode is switched from a high perveance state to a low perveance one.

In this paper, the circuit model for the beam generator was expanded to take into account grid capacitance and beam loss. Computer results based on the new circuit model predict a train of sinusoidal like pulses in the triode output when the grid is suddenly connected to a portion of the storage inductor. An electron beam generator, capable of producing a train of megavolt pulses at high currents, appears to be feasible.

ANALYSIS OF AN INDUCTIVE ENERGY HIGH PERVEANCE ELECTRON BEAM GENERATOR

Maurice Weiner
Electronics Technology and Devices Laboratory
USA Electronics R&D Command
Fort Monmouth, New Jersey 07703

Summary

Recently Slivkov and Dolgachev[1] proposed an interesting type of electron beam generator, consisting of a high voltage triode in series with a storage inductor. During the storage time the triode operates with a depressed collector voltage. A high energy current pulse is obtained when the triode is switched from a high perveance state to a low perveance one.

In this paper, the circuit model for the beam generator was expanded to take into account grid capacitance and beam loss. Computer results based on the new circuit model predict a train of sinusoidal like pulses in the triode output when the grid is suddenly connected to a portion of the storage inductor. An electron beam generator, capable of producing a train of megavolt pulses at high currents, appears to be feasible.

Introduction

In recent years much attention has been given to beam generators which utilize inductive energy storage. Compared to capacitive energy storage, inductive storage has an inherently large ratio of stored energy to weight. For applications which have a low weight requirement, therefore, inductive energy storage is an approach worth exploring.

In most beam generator designs considered previously, the operation was limited to either single shot or involved coercive pulsing, i.e., an external switching voltage was supplied for each output pulse. Less consideration has been given to the burst mode of operation, i.e., to the generation of a train of pulses. Unlike coercive pulsing, a switching voltage is required only to start and terminate the pulse train. The burst mode therefore places less stringent requirements on the switch, particularly when rapid pulsing at high power levels is sought.

Recently Slivkov and Dolgachev[1] proposed an interesting type of electron beam generator, consisting of a high voltage triode in series with a storage inductor. The triode operates with a depressed collector voltage. A foil window is provided at the anode end to extract the electron beam.

An attractive feature of this design has to do with the fact that the switch and beam accelerator functions are performed in the same structure. In previous designs utilizing inductive energy storage, the switch and accelerator functions were performed in separate components. Thus the new design is simpler and the system is made more compact.

The analytic treatment previously considered was geared toward single shot and coercive pulsing. In this paper the circuit model for the generator has been modified so as to allow for the existence of oscillations, i.e., the burst mode of operation. Computer results based on the new model clearly indicate that strong oscillations are present under a variety of conditions. Modifications in the generator design which are more suitable to the burst mode of operation, and to higher voltage operation, are discussed.

Basic Circuit Description

The basic circuit with no allowances for oscillations is shown in Figure 1. Initially a large voltage is placed on the grid. When the contact at B is closed, current will start to build up, resulting in energy storage in the inductors L_1 and L_2. During the storage interval the grid voltage will exceed the anode voltage. When the current has built up to a point close to its maximum value, signifying the end of the storage interval, the spark gap at P is fired. The grid potential is then suddenly reduced to the potential at the point of the tapped inductance. As a result of the reduced grid voltage, a large rate of change in the current will occur, accompanied by a build-up of voltage across the inductors, L_1 and L_2. This voltage will appear across the triode, producing the high voltage electron beam.

In the circuit of Slivkov and Dolgachev the voltage reduction is instantaneous since no allowances are made for grid capacitance. The circuit model also does not include the effect of beam losses. In this paper both grid capacitance and beam loss are incorporated into the circuit model.

Modified Circuit Model

The more detailed circuit model is shown in Figure 2, where the grid cathode capacitance C_g, and a resistance, R_g, shunt the inductor. R_g represents grid losses associated with beam interception and beam loading. Initially the grid cathode capacitance is charged to the voltage V_g. When the spark gap is fired current from V_c begins to flow in L_1. After a time roughly equal to L_1/R_c, where R_c is the charging resistance, the voltage across L_1, R_g, and C_g will significantly decrease and the grid cathode capacitance will start to discharge. This will be followed by oscillations in the grid voltage, associated with the L_1 C_g circuit. The oscillations in V_g will introduce corresponding variations in the triode impedance, which in turn will give rise to large variations in the inductive voltage. The inductive voltage oscillations then will appear across the triode. The oscillations will be affected by the losses given by R_g, Rc, as well as by the variation in voltage across L_1 induced by the changes in the primary current flowing in L_1.

Simple conditions under which oscillations will occur may be obtained as follows. In order for oscillations to occur, the fall time of the voltage across L_1 should be less than the period of oscillation. Thus $L_1/R_c \ll 2\pi (L_1C_g)^{1/2}$, or $R_c \gg (1/2\pi)(L_1/C_g)^{1/2}$. Similarly the grid resistance should satisy the condition $R_g \gg (1/2\pi)(L_1/C_g)^{1/2}$. In addition the oscillation period should be less than the fall time of the primary current. The fall time will be discussed later.

An alternative grid circuit for exciting oscillations is shown in Figure 3. Instead of using a bias voltage, the grid-cathode is pulsed during the storage interval. The pulse voltage is then removed at the same time that the spark gap is fired. If the fall time of the pulse is small compared to the period of oscillation, $2\pi(L_1C_g)^{1/2}$, the grid-cathode capacitance will be "shock" excited and grid oscillations will occur, which in turn will give rise to high voltage oscillations across the accelerator. The requirements that $R_g \gg (1/2\pi)(L_1/C_g)^{1/2}$, and that the oscillation period be less than the fall time of the primary current, also prevail.

In general, grid pulsing with a steep fall time will result in somewhat larger amplitude oscillations, compared to the bias mode where one has a finite R_c in the circuit. The two modes are equivalent when $R_c \to \infty$. Choosing a very large value R_c is prohibitive since this implies extremely large values of V_c at the same grid current levels. Another potential advantage of grid pulsing is that, after a pulse train has died out, little or no current flows through the spark gap and it is relatively easy to open up the grid circuit in preparation for generating another pulse train. The potential advantages of grid pulsing, however, must be balanced against the added circuit complexity needed to supply the grid pulse with a steep fall time.

Voltage Current Relationship in Triode

In order to obtain numerical results, the relationship among the grid voltage V_g, the anode-cathode potential, V_a, and the current, I, must be assumed. For this purpose the following is adopted:[2]

$$I = K\left(V_g + \frac{V_a}{\mu}\right)^{3/2} \qquad (1)$$

where K is the triode perveance and μ is the amplification factor. During the storage interval V_g is normally larger than V_a. If $V_g \gg V_a$, then Equation (1) reduces to the diode equation

$$I = KV_g^{3/2} \qquad (2)$$

When the switch is closed, however, it will no longer be true that $V_g \gg V_a$ since V_g may decline rapidly.

In order to demonstrate how the large voltage oscillations develop, it is instructive to solve Equation (1) for V_a,

$$V_a = \mu\left[\left(\frac{I}{K}\right)^{2/3} - V_g\right] \qquad (3)$$

Shortly before the spark gap is fired $\mu(I/K)^{2/3}$ and μV_g represents two large quantities whose difference is equal to the power supply voltage. When the spark gap is fired μV_g will undergo rapid oscillations while $\mu(I/K)^{2/3}$ will change slowly because of the energy storage in the inductive elements. Assuming V_g drops to about $V_g \simeq 0$, the magnitude of the voltage swing in V_a will be approximately μV_{go}, where V_{go} is the initial voltage on the grid. If we allow V_g to become negative, voltage peaks of $\simeq 2\mu V_{go}$ may be attained.

Circuit Response After Firing of Spark Gap at P

Computer results have been obtained for both the biased and pulsed grid cases. In particular, the variation in V_a and I as a function of time, subsequent to the firing of the spark gap, have been obtained. In obtaining the results for the acceleration interval the triode nature of the device is fully taken into account. Equations which govern the circuit, as well as the computer programs used for their solution, are discussed briefly in the Appendix.

Typical megavolt (MV) oscillations in V_a, for the biased grid case, are shown in the upper curve of Figure 4. The corresponding decline in the induction current, from which the energy for the oscillations is derived, is shown in the lower curve of Figure 4. Damping of the oscillations occurs when R_c, the charging resistance, is decreased. A similar damping occurs when the shunt resistance, R_g, is decreased. Eventually the current decays to a value determined by Equation (1) with $V_g = 0$ and $V_a = V_b$.

Computer results were obtained for various values of the tapped inductance, L_1. As expected, the pulse-width is narrowed by decreasing L_1. The narrower pulses usually are accompanied by an increase in amplitude, indicative of the wider swing in grid voltage permitted when L_1 is decreased.

Figure 5 shows that similar oscillations are present when the grid is pulsed. The parameters of Figure 5 are identical to those of Figure 4, except for the omission of V_c and R_c. An infinitely steep fall time is assumed. As mentioned previously, somewhat higher amplitude oscillations are expected for the pulsed grid case, because of the presence of R_c and the assumption of an infinitely steep fall time in the grid pulse.

Since the output voltage amplitude is $\simeq \mu V_g$, the required grid voltage may be decreased by increasing the amplification factor, μ. Figure 6 shows the MV oscillations which are present when $V_g = 100$ kV and $\mu = 10$, compared to the values $V_g = 390$ kV and $\mu = 2.5$ in Figures 4 and 5.

Fall Time

The fall time of the primary current may be approximated if we assume the current flowing through L_1 is equal to I, i.e., we ignore the currents in the secondary loops (Figure 2). Under these circumstances the differential equation governing the current is

$$V_b = (L_1 + L_2)\frac{dI}{dt} + \mu\left[\left(\frac{I}{K}\right)^{2/3} - V_g\right] \qquad (4)$$

The form of Equation (4) is identical to that of the diode if we regard the power supply voltage as

$$V_b' = V_b + \mu V_g \qquad (5)$$

and the diode perveance as

$$K' = \frac{K}{\mu^{3/2}} \tag{6}$$

The fall time constant, t_f, for the diode case is[1]

$$t_f = (L_1 + L_2)K' V_b'^{1/2} \tag{7}$$

Making use of Equations (5) and (6), the fall time for the triode is

$$t_f = \frac{(L_1 + L_2)K (V_b + V_g)^{3/2}}{\mu^{3/2}} \tag{8}$$

For the parameters listed in Figure 4, for example, $t_f \simeq 6.4\mu s$. Note that the fall time calculated from Equation (8) is in approximate accord with the exact computer results shown in the curves of Figure 4. As mentioned previously the oscillation period must be less than t_f in order to achieve large amplitude oscillations.

Inductive Storage Interval

During the storage interval it is important to know how quantities such as the current I, and anode-cathode potential, V_a, and the efficiency, η_s, vary with time, t. These quantities have been calculated previously[1] for the case of the vacuum diode, and are shown in Figure 7.

A similar calculation for the triode is complicated by the fact that, during the storage interval, Equation (3) does not apply. During the bulk of the storage interval, Equation (3) states that $V_a < 0$, which is contrary to fact if we assume the grid does not supply any appreciable energy to the beam. The reason for the discrepancy lies in the fact that Equation (3) does not account for the beam deacceleration in the grid-anode region. In order to accurately relate V_a to I and V_g, during the storage interval, a beam analysis should be undertaken.

A rough approximation of the storage behavior may be obtained, however, from the diode results. We adopt the view that V_g has the effect of increasing the effective perveance of the generator. For the same current, I, and anode-cathode voltage drop, V_a, one has

$$I = K_e V_a^{3/2} = K\left[V_g + \frac{V_a}{\mu}\right]^{3/2} \tag{9}$$

and

$$K_e = K\left[\frac{V_g}{V_a} + \frac{1}{\mu}\right]^{3/2} \tag{10}$$

where K_e is the equivalent perveance of the diode and V_a is evaluated at the end of the storage interval. As an example, K_e may be evaluated for the parameters listed in Figure 4. Making use of Equation (10), $K_e = 160 \times 10^{-6}$ perveance. From Figure 7, at I = 1000A, the storage time is $\simeq 233\mu s$, at which point 38 percent of the maximum storage current and 52 percent of the maximum anode-cathode voltage is achieved. The storage efficiency is approximately 58 percent at this point in time.

A general expression for the storage time constant t_r, analogous to L/R, is given by $(L_1 + L_2)K_e V_b^{1/2}$. The time constant for the aforementioned example is 408 μs, indicating we have chosen to fire the spark gap before t_r. Choosing to fire the spark gap at a time much larger than the time constant is wasteful of energy, since the efficiency is low and little gain in energy storage is achieved. On the other hand, choosing a firing time much less than the time constant, although highly efficient, may not provide sufficient storage energy.

Periodic Focusing

The use of a single control electrode is probably not the optimum type of structure to achieve MV pulses at high beam currents. In order to avoid breakdown a fairly large anode-cathode space is needed. Given such a large space the transmission of the beam current with only a single grid is difficult to achieve without heavy beam losses, caused by space charge effects. One possible means for overcoming this problem is to use a quasi-periodic electrostatic focusing[3], as shown in Figure 8. The grids alternate in potential during the storage interval. One set is connected to a high grid potential. The other set is connected to various points on the inductor. When the spark gaps are activated, the grid potentials are suddenly reduced, giving rise to a large rate of current change, which in turn produces a high voltage burst of beam current. If all the acceleration grid voltages are switched simultaneously then the total change in grid voltage will be $n V_g$ where V_g is the voltage applied to each grid, with respect to its adjacent electrode. n is the total number of grids. The amplitude of the output voltage will then be $n\mu V_g$. The circuit equivalent may be considered that shown in Figure 9.

Trajectory calculations for a planar beam in the presence of such a periodic potential indicates fair transmission, approximately 80 percent.[3] No trajectory results have been obtained for the case of a cylindrical beam, however. In addition, no trajectory results were obtained which apply to the acceleration interval. This is a particularly important area of investigation since there exists the possibility that the beam will blow up during the acceleration time, thereby reducing the beam transmission.

Heating of the Anode Foil

Heating of the foil will present severe problems. Suppose a design corresponds to the parameters of Figure 4, and that a 1 mil thick gold foil with a 20 cm^2 area is chosen for the anode. At one mil thickness the 1 MV electrons will pass through the foil largely unattenuated while the storage state electrons will be absorbed. A beam area of 20 cm^2 is chosen since, for a current of 1000 amps, the cathodes now available yield current density of $10A/cm^2$.

By the end of one storage interval the beam will have delivered energy to the foil in the amount

$$\tfrac{1}{4}(L_1+L_2)\, I^2(1-\eta_s)/\eta_s .$$

For the previous example $\eta_s = 0.58$, $L_1 + L_2 = 10^{-2}H$,

and $I = 10^3$ amps, so that the energy dissipation in the foil is 3600 joules, assuming all the beam energy is absorbed. Assuming that no heat is conducted or radiated away during the storage interval, 233μs, the foil will attain a flash temperature of about 28,000 °C. Although the actual temperature will be much lower because of heat losses, the example is indicative of the severe heating problem one may expect. One possible approach is a trade-off which reduces the storage energy. For example, using 10^{-3}H instead of 10^{-2}H, will reduce the calculated temperature by an order of magnitude, although the droop in the oscillation will be increased.

A more desirable technique for reducing foil dissipation involves defocusing of the beam during the storage state, so that the beam does not strike the foil but is instead collected by adjacent electrodes able to withstand the dissipation (Figure 10). During the acceleration state the beam is focused into the foil. The focusing may be accomplished, possibly, by proper design of the electrostatic control grids, so that during acceleration the high voltage automatically refocuses the beam onto the foil. The focusing may be aided perhaps by a pulsed longitudinal magnetic field which is introduced shortly before the start of the acceleration cycle.

Conclusions And Recommendations

A circuit analysis was performed on a beam generator design utilizing inductive energy storage. The design resembles that of a triode with a depressed collector anode. The results of the analysis indicated that MV pulse trains at high current levels will occur. The analysis also strongly suggests that such oscillations will occur in a multi-gridded structure having a periodic potential. The multi-gridded structure will allow the extension to higher acceleration voltages.

Suggested areas for further design study include the following:

1) A beam trajectory study for the periodic potential should be undertaken to determine the quality of transmission. High levels of beam transmission are required in order for the oscillations not to damp out. Such a study also will dictate the choice of circuit parameters and the dimensions of the structure.

2) The concept of defocusing the beam at the anode during the storage interval should be incorporated into the beam trajectory analysis. As mentioned previously, defocusing the beam will ease the thermal dissipation problems associated with the window.

3) Design consideration should be given to mimimizing the voltage drop across the accelerator during the storage interval, while maintaining high current levels. This means resorting to a structure with a large effective perveance. A lower voltage drop will make the concept compatible with voltage generating machines, which are capable of supplying high currents at a few kV.

4) The use of supercooled inductors should be considered in the design. At low impedance levels the resistive losses in the storage inductors should be as low as possible in order to take advantage of the concept of inductive-energy storage.

5) Consideration must be given to the technique which will be used to open up the grid circuit after each burst of oscillations. As mentioned previously the problem is lessened in the grid pulsing case. One possible approach is the placement of a repetitive series interrupter (RSI) in the grid circuit.

6) In order to obtain reasonably small diameter beams, fairly large current densities are required. A cathode study must be undertaken to determine whether such cathodes are feasible. Large convergence ratio cathodes may be one approach for obtaining the high current density levels.

Appendix

The loop equations for the circuit of Figure 2 are:

$$V_b = V_a + L_1 \frac{d\,(I-I_2-I_3-I_4)}{dt} + L_2 \frac{dI}{dt} \qquad (A1)$$

$$L_1 \frac{d\,(I-I_2-I_3-I_4)}{dt} = I_2 R_g \qquad (A2)$$

$$I_2 R_g = V_g \qquad (A3)$$

$$I_2 R_g = V_c + I_4 R_c \qquad (A4)$$

$$L_1 \frac{d^2\,(I-I_2-I_3-I_4)}{dt^2} = \frac{dI_2}{dt} R_g \qquad (A5)$$

$$\frac{dI_2}{dt} R_g = \frac{dI_4}{dt} R_c \qquad (A6)$$

$$\frac{dI_2}{dt} R_g = \frac{I_3}{C_g} \qquad (A7)$$

V_a is given by

$$V_a = \mu \left[\left(\frac{I}{K} \right)^{1/1} + V_g \right] \qquad (A8)$$

where V_g is replaced by $-V_g$ because of the sign convention of the circuit. The initial conditions are:

$$I = I_o \quad \text{(A9)}$$

$$I_3 = 0 \quad \text{(A10)}$$

$$I_4 = -I_2 = V_c/(R_c + R_g) \quad \text{(A11)}$$

Equations (A1) - (A8) were solved by an iterative procedure using a Burroughs 5500 computer. The computer program employed a Runge-Kutta-Nystrom starting procedure followed by the Hamming method. Details of the programs are found elsewhere.[4]

References

1. I. Slivkov, G. Dolgachev, "Accelerating and Switching Optoelectronic Systems of a High Powered Acceleration with an Inductive Element, Prib. i Tekh. Eksper, No. 3, pp. 27-30, 1975.

2. K. Spangenberg, Vacuum Tubes, McGraw Hill, New York, New York, 1948.

3. A. Koslov, A. Maslov, G. Prokhova, I. Slivkov, " A Multelectrode Electron-Optic System with an Inductive Storage Device for a High-Current Accelerator", Prib. i. Tekn Eksper., No. 3, pp. 25-27, 1975.

4. A. Pixley, A. Macek, "A B5000 ALGOL 60 Program for the Solution of a System of First Order Differential Equations (Hamming Method)", Burroughs Technical Bulletin MRS-126, Feb 1964.

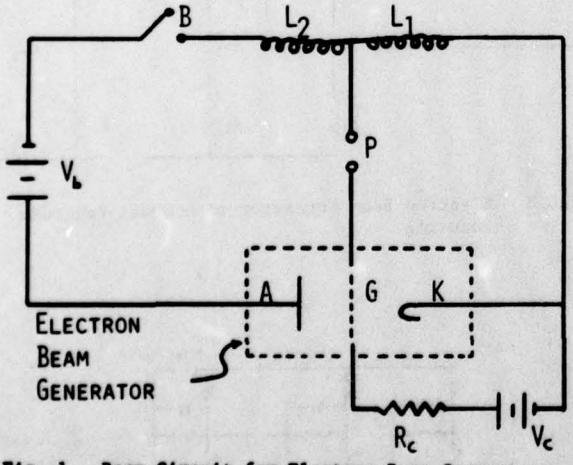

Fig. 1 Beam Circuit for Electron Beam Generator Utilizing Inductive Energy Storage.

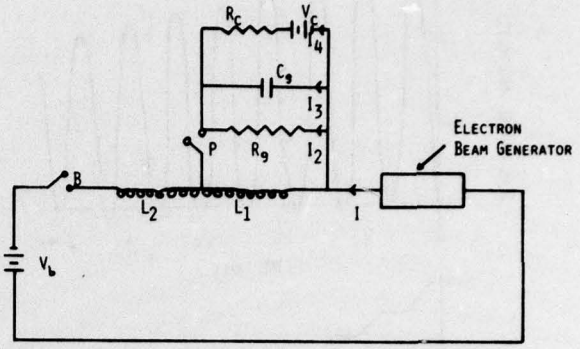

Fig. 2 Circuit Model of Electron Beam Generator Utilizing Inductive Energy Storage. Model Includes Grid Capacitive Effects and Beam Loss.

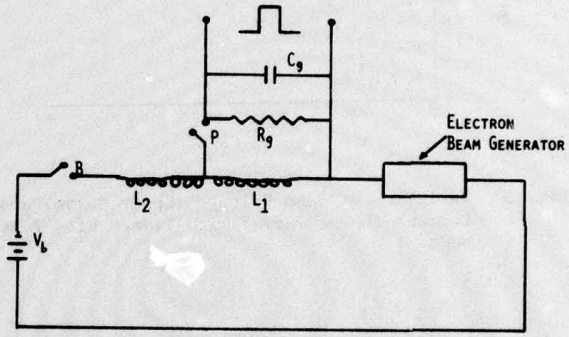

Fig. 3 Circuit Model of Electron Beam Generator Utilizing Inductive Energy Storage. Model Includes Capacitive Effects and Beam Loss. Grid Pulsed During Storage Interval.

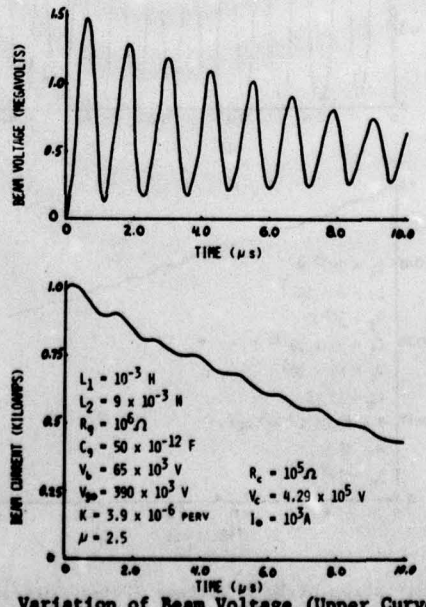

Fig. 4 Variation of Beam Voltage (Upper Curve) and Current (Lower Curve) with Time. Grid Bias Mode.

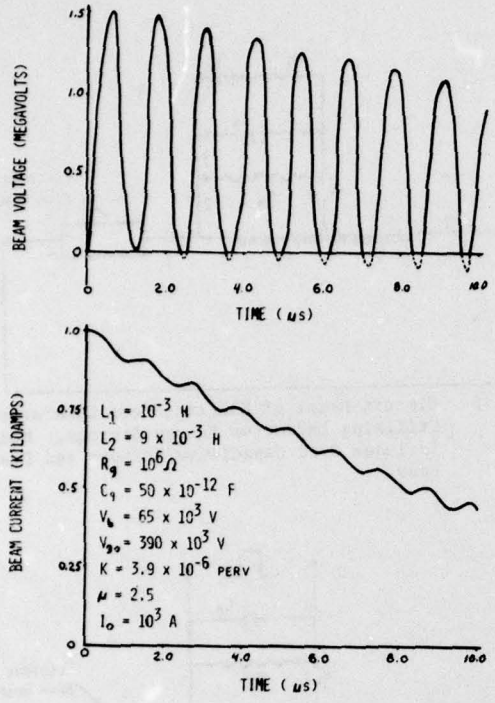

Fig. 5 Variation of Beam Voltage (Upper Curve) and Current (Lower Curve) with Time. Grid Pulse Mode.

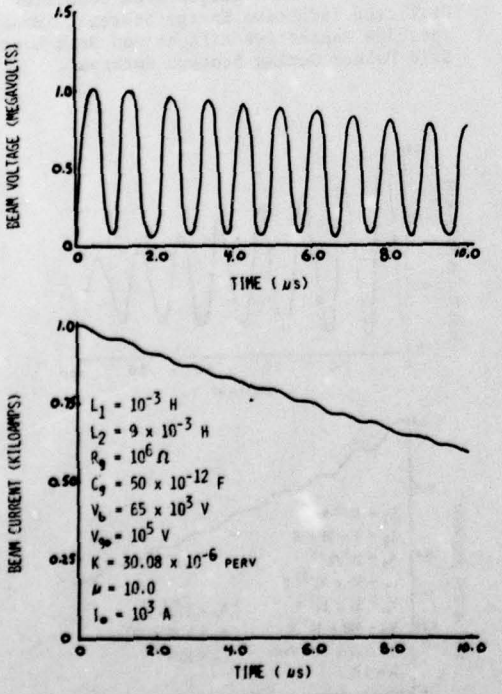

Fig. 6 Variation of Beam Voltage (Upper Curve) and Current (Lower Curve) with Time. Grid Pulse Mode.

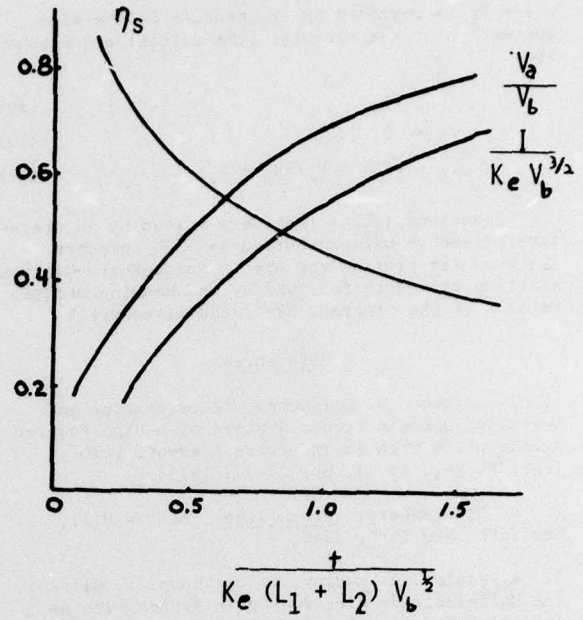

Fig. 7 Diode Dependence of Current, Voltage and Efficiency with Time (Ref. 1)

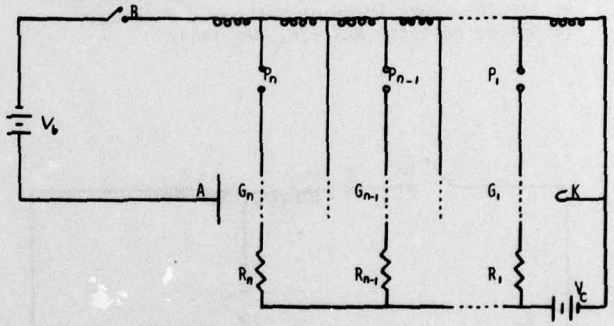

Fig. 8 Electron Beam Generator with Quasi-Periodic Focusing.

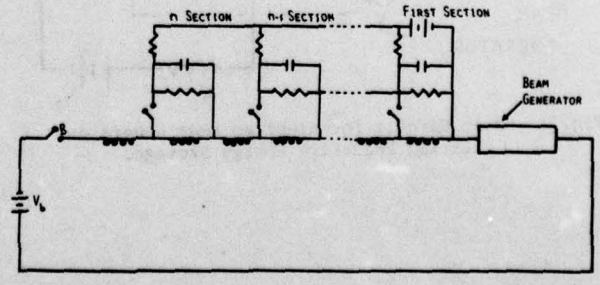

Fig. 9 Circuit Model of Beam Generator with Quasi-Periodic Focusing.

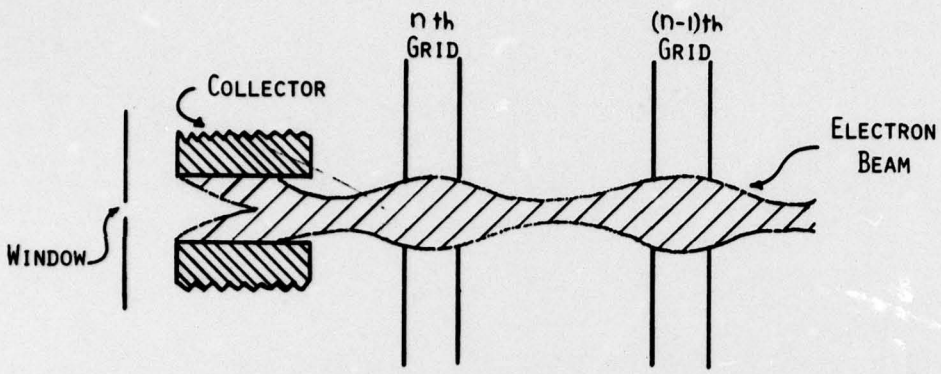

Fig. 10 Defocusing of Electron Beam During Storage Cycle.